Lawrence Berkeley National Laboratory
LBL Publications

Title
LOW ENERGY ELECTRON DIFFRACTION STUDIES OP THE ADSORPTION OF UNSATURATED HYDROCARBONS AND CARBON MONOXIDE ON THE PLATINUM (111) AND (100) SINGLE CRYSTAL SURFACES

Permalink
https://escholarship.org/uc/item/8x1360k7

Authors
Morgan, A.E.
Somorjai, G.A.

Publication Date
1969-03-01

LOW ENERGY ELECTRON DIFFRACTION STUDIES OF THE ADSORPTION
OF UNSATURATED HYDROCARBONS AND CARBON MONOXIDE ON
THE PLATINUM (111) AND (100) SINGLE CRYSTAL SURFACES

A. E. Morgan and G. A. Somorjai

March 1969

LAWRENCE RADIATION LABORATORY

UNIVERSITY of CALIFORNIA BERKELEY

DISCLAIMER

LOW ENERGY ELECTRON DIFFRACTION STUDIES OF THE ADSORPTION OF UNSATURATED HYDROCARBONS AND CARBON MONOXIDE ON THE PLATINUM (111) AND (100) SINGLE CRYSTAL SURFACES

A. E. Morgan and G. A. Somorjai

Inorganic Materials Research Division, Lawrence Radiation Laboratory,
and Department of Chemistry,
University of California, Berkeley, California

ABSTRACT

The interaction of simple aliphatic hydrocarbons and carbon monoxide with Pt(111) and Pt(100) surfaces, at gas pressures $\leq 1 \times 10^{-7}$ torr, has been studied using low energy electron diffraction (LEED), mass spectrometry, flash desorption and work function (ϕ) measurements. The Pt(111) substrate was characterized by a (1×1) diffraction pattern while a (5×1) surface structure was visible on Pt(100). In contrast to the saturated hydrocarbons, all the other gases used (CO, C_2H_2, C_2H_4, C_3H_6, 1,3-butadiene and the isomeric butenes) were readily chemisorbed on both substrates. Relatively large decreases in ϕ resulted from the chemisorption of the unsaturated hydrocarbons while a small increase in ϕ was measured due to the adsorption of CO. All gases were held in one bonding state except for CO which exhibited three bonding states on the (100) surface.

A (2×2) surface structure was produced on the (111) face by all of the unsaturated hydrocarbons studied with the exception of isobutylene which exhibited longer range ordering. C_2H_2 and C_2H_4 produced a c(2×2) structure on the (100) face of platinum. The adsorption of the other hydrocarbons however, generated no extra features in the (100) diffraction pattern, i.e. there was no indication of ordering. The necessity of close packing of the olefins appeared to be responsible for the presence of ordered structures on the Pt(111) surface and for

their absence on Pt(100). The results of these structural studies indicate that the carbon atoms are sp^2 hybridized in the adsorbed state. The chemisorption of CO resulted in the appearance of a (4×2) structure on both (111) and (100) surfaces. This structure was transformed by electron beam desorption into a (3×3) structure on the Pt(100) surface.

I. INTRODUCTION

Few reactions in surface chemistry have received more attention than the hydrogenation of unsaturated hydrocarbons over transition metal catalysts. Although a great deal of data are available,[1] the reaction mechanisms remain elusive. Since it has been clearly established[1] that the adsorption of an unsaturated hydrocarbon on the metal surface precedes its hydrogenation, studies of the interaction of these hydrocarbons with metal surfaces are necessary precursors to an understanding of the reaction mechanisms. Low energy electron diffraction (LEED) permits such studies to be made using well-defined, single crystal metal surfaces under carefully controlled experimental conditions. Mass spectrometric, work function and flash desorption techniques can be conveniently combined with LEED measurements to complement the diffraction data.

Platinum is one of the most widely-used metals for catalytic hydrogenation reactions. Since the (110) face facets above 600°C,[2] the (100) and (111) faces were chosen to examine how the structure of the metal surface influences the chemisorption process. Carbon monoxide, a major constituent of the ambient in a stainless steel ultra high vacuum (UHV) system, readily chemisorbs on platinum substrates forming ordered surface structures.[3] It often competes with other gases for adsorption sites or even displaces some of the more weakly-held molecules on a catalyst surface. Therefore the interaction of CO with the Pt surfaces was first examined to distinguish these surface structures from those formed by hydrocarbon chemisorption.

The gaseous unsaturated hydrocarbons used were acetylene (C_2H_2), ethylene (C_2H_4), propylene (C_3H_6), 1-butene $(C_2H_5CHCH_2)$, cis- and trans-2-butene $(CH_3CHCHCH_3)$, isobutylene $((CH_3)_2CCH_2)$ and 1,3-butadiene

$(CH_2CHCHCH_2)$. By varying the substituent alkyl groups around the olefin

double bond in this manner, the geometric and steric influences on olefin

chemisorption could be studied. Electronic effects due to the electron

donating or withdrawing properties of the substituents were examined by

measuring the change in the work function of the metal surface during

chemisorption.

II. EXPERIMENTAL PROCEDURE

The experimental procedures have been described previously.[4] Sum-

marizing briefly, a Varian post-acceleration LEED apparatus was utilized,

along with a quadrupole mass spectrometer to monitor flash desorption

species. Work function changes due to gaseous adsorption were measured

by the contact potential difference method using the LEED electron gun

itself.[5] During the adsorption studies, a steady state hydrocarbon flux,

corresponding to virtual pressures of 10^{-9}-10^{-7} torr, was flowing through

the diffraction chamber to minimize the generation (and hence chemisorption)

of CO.[4] The substrates were maintained near room temperature since crack-

ing of adsorbed hydrocarbons became appreciable at elevated temperatures.

III. RESULTS

A. The Structures of the Platinum Substrates

Diffraction patterns were obtained from both the (100) and (111)

surfaces by mere anneal of the crystals in UHV. Rings[2,4] were visible

on both patterns; these result from randomly-oriented domains of carbon on the

substrates. The diffraction characteristics of the rings indicate that the carbon

was present as graphite with the basal plane parallel to the substrate.

Ion bombardment using high purity argon, followed by high temperature

anneal, improved the overall quality of the diffraction patterns but the rings remained visible. These were ultimately removed by heating the crystals at 1000°C in 1×10^{-5} torr oxygen.[4]

The diffraction patterns of the carbon-free substrates are shown in Fig. 1. The pattern of the (111) surface (Fig. 1a) is typical for that of a fcc crystal whose bulk structure is maintained at the surface. No extra spots, indicative of a reconstruction of the surface atoms, were present. However the pattern of the (100) surface (Fig. 1b) was far from simple; 1/5th order diffraction spots were present along the x- and y-axes (or sometimes along only one axis) initially suggesting two domains of (5X1) periodicity. Using the matrix formulation,[6] this structure is generated in real space by two sets of unit mesh vectors, $\vec{i}$ and $\vec{j}$, whose components are given by the rows of the transformation matrices, $A = \begin{vmatrix} 5 & 0 \\ 0 & 1 \end{vmatrix}$ and $B = \begin{vmatrix} 1 & 0 \\ 0 & 5 \end{vmatrix}$. These unit mesh vectors are defined relative to the substrate unit mesh. However, from lack of a more complete description, the structure will be referred hereafter to Pt(100)-(5X1).

Providing that the surface carbon had been completely removed, the (5X1) structure was stable at all temperatures ($\leq 1400°C$) used in these experiments. The structure has also been observed[7,8] on the (100) face of gold, which directly follows platinum in the periodic table. Structurally, there is very little difference between gold and platinum, but their electronic properties (magnetic susceptibility, electrical conductivity, etc.) are substantially different since gold has a filled d-electron shell while platinum has unpaired d-electrons. Moreover, there are also dramatic differences between the catalytic properties of the metals. Auger spectroscopy studies on both Pt(100)[9] and Au(100)[10]

surfaces failed to detect a stabilizing impurity for the surface structure suggesting that it is characteristic of a clean surface. Fedak and Gjostein[11] proposed a coincident site model for the gold structure consisting of a hexagonal surface layer superimposed on the square Au(100) substrate. Using this model,[12] limited success was achieved in trying to reproduce the LEED pattern by the method of optical simulation.[13] However, these ideas assume the validity of a kinematic scattering model and hence their plausibility is questionable. Thus, at the moment, a complete description of the atomic arrangements at the Pt(100) and Au(100) surfaces is lacking.

2. Adsorption of Carbon Monoxide

Carbon monoxide readily chemisorbs on the Pt(100) substrate causing the 1/5th order diffraction spots to rapidly disappear.[4] The intensities of the integral order spots increased during the initial stages of CO chemisorption as the extra spots disappeared. Continued adsorption of CO then caused a gradual decrease in the intensities of the remaining (1×1) diffraction spots until new diffraction features appeared. Figure 2(a) illustrates schematically the diffraction pattern visible after the adsorption of CO had reached saturation at room temperature. The extra spots were less intense and more diffuse than the (1×1) diffraction spots. They were visible only at incident beam voltages $E < 150$ V and reached their maximum intensities at $E = 15$ V and 90 V. The pattern is indicative of domains of a (4×2) unit mesh rotated at 90° to each other. The transformation matrices giving the components of the new unit mesh in real space, referred to the substrate mesh, are

$$A = \begin{vmatrix} 1 & -2 \\ -2 & 0 \end{vmatrix} \text{ and } B = \begin{vmatrix} 2 & -1 \\ 0 & 2 \end{vmatrix}.$$

The Pt(100)-(4×2)-CO structure was stable in vacua provided that the crystal was turned away from the electron gun. However, if the electron beam was allowed to strike the surface for a few minutes, the more weakly bonded CO(α_1-CO) was desorbed and the diffraction pattern changed; the extra diffraction spots first became streaky, then those along the x- and y-axes disappeared leaving very faint and ill-defined extra spots [Fig. 2(b)]. The pattern now suggests the presence of (3×3) unit meshes with transformation matrices $A = \begin{vmatrix} 1 & -2 \\ 1 & 1 \end{vmatrix}$ and $B = \begin{vmatrix} 2 & 1 \\ -1 & 1 \end{vmatrix}$. Flash desorption studies showed that the binding of the CO(α_2-CO) to the surface was only slightly stronger, the relevant desorption temperatures being 130°C for α_1-CO and 170°C for α_2-CO.

A small amount of CO(β-CO) remained on the surface above 200°C; this was characterized by a (1×1) diffraction pattern and a flash desorption temperature of 600°C. When all the CO was desorbed by heating the crystal above 600°C, the usual (5×1) surface structure of clean platinum readily reappeared.

The chemisorption of CO on the Pt(111) surface at room temperature gave rise to the diffraction pattern shown schematically in Fig. 3. Once again, the extra features were fainter and more diffuse than the "normal" spots. The former were most clearly visible at E = 19 V, 76 V and 110 V. The 1/2 order spots were weak relative to the 1/4 order spots. The pattern again suggests a (4×2) unit mesh, with domains at 60° to each other and with transformation matrices $A = \begin{vmatrix} 1 & 2 \\ 2 & 0 \end{vmatrix}$, $B = \begin{vmatrix} 2 & 1 \\ 0 & -2 \end{vmatrix}$ and $C = \begin{vmatrix} 1 & 1 \\ 2 & -2 \end{vmatrix}$. The pattern was stable in vacua; the extra features became slightly more diffuse, and tended to streak and coalesce under the influence of the electron beam but no new surface structure was apparent. The flash desorption spectrum showed a large m/e = 28 (α-CO) peak centered at 170°C but no resolution into α_1- and α_2-CO was achieved. No other peaks

were detected suggesting the absence of a more strongly chemisorbed form
of CO. Also all extra diffraction features vanished above 170°C; the
diffraction pattern gave no indication of CO adsorption above this
temperature.

C.   Adsorption of Unsaturated Hydrocarbons

The diffraction pattern, shown in Fig. 4(a), resulted from the chemi-
sorption of acetylene, ethylene , propylene, 1-butene, cis-2-butene,
trans-2-butene and 1,3-butadiene on the Pt(111) substrate. There are
sharp 1/2 order spots which are visible throughout the entire beam voltage
range (0-250 V) although somewhat fainter than the (1×1) diffraction
spots. They were most intense at $E = 17$ V and 55 V. The pattern indicates
that a (2×2) surface structure had been formed (transformation matrix
$\begin{vmatrix} 2 & 0 \\ 2 & 2 \end{vmatrix}$). The structures were stable in vacua and not affected by the
electron beam.

Two experimental criteria were necessary to ensure the generation of
the (2×2) pattern; a) the cleanliness of the surface. If carbon was pre-
sent on the substrate, as indicated by the appearance of rings in the
diffraction pattern, no extra diffraction features were generated by
hydrocarbon chemisorption. After an unsaturated hydrocarbon had been
adsorbed and then desorbed a few times, rings were visible in the pattern
indicating some cracking of the adsorbate. The surface was then cleaned
by high temperature treatment in oxygen. Also, since CO was frequently
preferentially chemisorbed on the Pt substrates in competition with the
olefin, the surface was cleaned by flashing the crystal to 800°C immediately
before introducing the hydrocarbon; b) slight heating of the Pt crystal
was required to order the chemisorbed hydrocarbon. If the gases were

introduced into the diffraction chamber with the Pt substrate at room temperature, the pattern background increased but no extra features resulted. However, if the crystal was then heated at 100°C for a few minutes, the 1/2 order spots appeared, initially diffuse but gradually becoming sharper.

Isobutylene was the only unsaturated hydrocarbon whose chemisorption did not give rise to the (2×2) surface structure. The gas was readily chemisorbed causing an increase in the pattern background. Extremely faint (1/5, 1/5) order spots were sometimes visible around the (00) spot but sufficient detail to identify a surface structure was lacking.

The flash desorption spectra of all the chemisorbed hydrocarbons were similar. The hydrocarbon desorbed around 140°C while hydrogen peaks were detectable around 200°C and 340°C. If the crystal was cooled < 200°C in the presence of a hydrocarbon, the (2×2) surface structure first appeared at a substrate temperature of approximately 130°C. The surface structures were easily removed by heating the crystal to 150°C.

The chemisorption of acetylene and ethylene on the Pt(100) substrate first caused a rapid disappearance of the (5×1) surface structure. Then extra spots of half integral indices appeared at the center of each Pt reciprocal unit mesh [Fig. 4(b)], indicating the formation of a C(2×2) surface structure (transformation matrix $\begin{vmatrix} 1 & 1 \\ 1 & -1 \end{vmatrix}$). Although fainter than the (1×1) diffraction spots, these were visible at all beam voltages used (0-250 V) and were most intense at E = 16 V, 42 V, 96 V and 155 V. The same experimental conditions were necessary to the generation of the C(2×2) surface structure as were employed during the formation of the Pt(111)-(2×2)-structure. Again, cracking of adsorbed hydrocarbons eventually contaminated the substrate.

Chemisorption of propylene, cis-2-butene, trans-2-butene and

1,3-butadiene produced a (1×1) diffraction pattern with no indication

of any extra features. During the initial stages of hydrocarbon chemi-

sorption, the intensities of the integral order spots increased as the

1/5 order spots disappeared. Continued adsorption caused a gradual re-

duction in the intensities of all of the diffraction features and an

increase in pattern background. However, after isobutylene had chemi-

sorbed to saturation, the (5×1) surface structure was still clearly

visible along with very faint, broad streaks, parallel to the x- and

y-axes, at 1/3 positions. There were no discernible differences in the

rates of hydrocarbon chemisorption from those observed on the (111)

substrate. Also, the flash desorption spectra were similar to those

obtained previously. By heating the crystal to 150°C, the hydrocarbons

were desorbed and the (5×1) surface structure reappeared.

D. Work Function Changes

The changes in the work function, ϕ , (error ±0.02V) of the

metal substrates due to gaseous chemisorption are summarized in Table I,

along with the surface structures formed.

The chemisorption of CO caused an increase in the work function, ϕ,

while chemisorption of an unsaturated hydrocarbon always resulted in a

decrease in the work function of the (111) and (100) surfaces of

platinum. If carbon was present on the substrate (as indicated by the

ring-like diffraction pattern), the work function change upon chemi-

sorption was appreciably reduced. In order to minimize possible surface

contamination by carbon monoxide and hence to achieve greater repro-

ducibility of the $\Delta\phi$ values, the work function measurements were made

as follows; the crystal was first flashed to 800°C to remove chemisorbed CO. When the sample had cooled to about 150°C, the hydrocarbon was introduced at a pressure of about 1×10^{-8} torr. Within 1-2 minutes, the chemisorption had reached saturation as indicated by no further change in ϕ. The diffraction pattern was then examined to ascertain the surface structure formed.

$\Delta\phi$ was independent of the hydrocarbon pressures used in these studies ($\leq 1 \times 10^{-7}$ torr). However, as the crystal remained in vacua, a slight increase in ϕ was observed due to a gradual adsorption of residual CO. In one experiment, cis-2-butene was adsorbed to saturation on the Pt(111) surface producing the (2×2) surface structure and $\Delta\phi$ equalled -1.31 eV. CO was then introduced into the diffraction chamber at 4×10^{-8} torr. After about 2 hours, the extra spots had disappeared and ϕ was slightly greater than that of the clean surface. However, the Pt(111)-(4×2)-CO pattern was not generated. Conversely, CO was first adsorbed to saturation on the (111) surface ($\Delta\phi = + 0.17$) and then cis-2-butene introduced at 2×10^{-8} torr. A very slight decrease in ϕ was noted but the (4×2) surface structure was not removed.

Finally, saturated gaseous hydrocarbons, methane, ethane, and n-butane at temperatures up to 700°C and at gas pressures in the range of 10^{-9} to 10^{-7} torr did not seem to chemisorb on the Pt(100) and Pt(111) faces. The surface structures and work function increases characteristic of adsorbed CO were slowly formed, with the substrate at room temperature. Thus, this apparent absence of chemisorption of the paraffins on the platinum surfaces could result from preferential CO chemisorption.
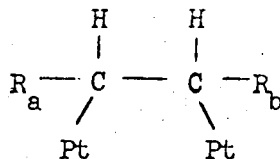
IV. DISCUSSION

The relative ease of desorption of the adsorbed molecules which were studied, their large size (with the exception of C_2H_4 and C_2H_2) indicate that their chemisorption does not involve replacement of the platinum atoms (reconstruction). The correct identification of the new unit mesh from the extra diffraction beams which appear during adsorption, however, in the absence of detailed intensity analysis, does not lead to a unique assignment of the position of the adsorbate molecules on the surface. For example the (2×2) diffraction pattern can be generated[14] by at least eight simple arrangements of the adsorbed species on the (111) face of a fcc metal. The results of other measurements (work function, flash desorption, etc) geometric and steric arguments and chemical intuition, must be used to reject the more unlikely arrangements.

One of the striking results of this study is the discovery that almost all of the chemisorbed C_2-C_4 olefins form ordered surface structures on the Pt(111) surface while there is no indication of ordering of these molecules (with the exception of C_2H_4) on the (100) face of platinum. Work function measurements indicate that there is not much difference between the amounts of adsorbed gas on the two substrates. A model will be proposed which, in addition to explaining other data, shows that close packing of the adsorbed molecules on the Pt(111) surface which exhibits three-fold symmetry gives rise to a preferred arrangement and hence, an ordered surface structure. The two fold symmetry of the (100) surface allows the adsorption and close packing of different olefins in several arrangements, all of which are equally probable and lead to the same surface coverage. Thus, ordering of the adsorbed molecules into one type of surface structure does not take place.

A. Chemisorption of the Unsaturated Hydrocarbons

There are two basic structures proposed,[1] for an adsorbed olefin,

an σ-diadsorbed and a π-adsorbed configuration. A σ-diadsorbed olefin

is formed by sp^3 hybridization of the olefinic carbon atoms and by the

formation of two σ bonds between the carbons and two metal atoms; i.e.

$$R_a - \overset{\displaystyle H}{\underset{\displaystyle Pt}{\overset{|}{\underset{/}{C}}}} - \overset{\displaystyle H}{\underset{\displaystyle Pt}{\overset{|}{\underset{\backslash}{C}}}} - R_b$$

Alternatively, it is proposed[1] that any olefin may form a π-donor bond

with a surface metal atom. As the carbon atoms are still sp^2-hybridized,

the groups attached to the carbon atoms are almost coplanar in a plane

parallel to the surface. The presence of π-adsorbed olefins on the platinum

substrates is indicated by the observed decreases in the work function

showing that the π-electron system of the adsorbate is electron deficient;

increases in the work function would be expected for σ-diadsorbed olefins

using electronegativity considerations. That the adsorbed olefins retain

their sp^2 hybridization is also indicated by the adsorption characteristics

of acetylene and ethylene on the platinum surfaces. From consideration

of the geometry of a σ-diadsorbed hydrocarbon on fcc metals, (tetrahedral

bond angles), it follows[15] that acetylene should only adsorb on surfaces

which provide the larger interatomic spacings (e.g. on the (100) and (110)

orientations) but not on the (111) face, whereas σ-diadsorbed ethylene

may adsorb on either surface [(111) or (100)] across the shorter inter-

atomic spacing (2.77Å). However, acetylene and ethylene adsorbs readily

on both the (100) and (111) platinum substrates as they should if they

retained their π-bonding characteristics. The ligand field theory, which has

been applied to explain bonding of adsorbed molecules on transition

metal surfaces[16-18] regards the adsorbent metal atom as the central atom

in a complex where the surrounding metal atoms and the chemisorbed molecule

are the ligands. Although a reasonable description of the binding of an

olefin (as either the σ-diadsorbed or π-adsorbed species) at the (100)

surface of a fcc metal can be achieved using this model, no simple analogy

is available for binding a hydrocarbon residue to the (111) surface since

no orbitals emerge normal to the surface.[17] Also, this molecular orbital

model is inadequate for a description of a π-adsorbed alkyne on the (100)

surface of a fcc metal since there are no surface orbitals available to

bind the alkyne by both its π-orbitals simultaneously. The application

of the results of ligand field theory to surface atoms which are in a

highly asymmetric environment can also be questioned. Thus an adequate

description of the adsorption sites on a metal surface is lacking.

Nonetheless, the model of a π-adsorbed olefin on the (100) surface,

proposed by Bond,[17] will be adopted (Fig. 5). The bonding, Fig. 5(a),

involves 1) a σ-bond formed by electron donation from the filled bonding

orbital of the olefin to the metal's e_g orbital and possibly, 2) a π-bond

formed by back donation from the t_{2g} orbitals into the vacant π-antibonding

orbitals of the olefin. This tends to reduce the accumulation of negative

charge on the metal atom. The Pt(100) substrate is represented in Fig. 5

by the usual square array of surface atoms, since the (5×1) surface

structure converts to (1×1) during the adsorption of most olefins. Figure

5(b) is a scale diagram of the close packing of chemisorbed ethylene; the

Pt-Pt near neighbor distance, a, is 2.77Å while the dimensions of the

adsorbate molecule are taken to be those of gaseous ethylene [C=C 1.34Å,

C-H 1.07Å, ∢HCH ~ 120°]. The unit mesh is a centered square of side, 2a,

and the fractional coverage θ (defined as the ratio of the number of ad-

sorbate molecules to the number of substrate atoms) is 1/2. The observed

decrease in the work function, φ, indicates that the electron donation

from adsorbate to metal is not fully compensated by back donation into

the antibonding orbitals of the adsorbate.

The disordered chemisorption of propylene, resulting from the random

filling of the adsorption sites, is depicted in Fig. 6 [C-C 1.51Å]. The

molecule can take up several orientations, all equally probable, on the

(100) platinum surface. Presumably, the adsorbed molecules would not

rotate into preferred alignments due to the close packing and thus, the

LEED pattern displays no extra features. The surface coverage, θ, is

still 1/2 and hence the larger decrease in φ observed with propylene

(-0.28 V) when compared to ethylene must reflect the influence of the

methyl group. Similar arguments apply to the packing of cis-2-butene;

in this case, θ is slightly less than 1/2 and the further decrease of

-0.31 V in φ when compared with propylene can be acribed to the presence

of the second methyl group. The more open structures of isobutylene and

trans-2-butene will probably reduce the coverage still further and this

can account for the smaller changes in the work function than that observed

with cis-2-butene. The different work function changes observed for the

adsorption of the cis- and trans-butene (-1.34 V and -1.12 V, respectively)

indicate that the adsorbate molecules did not isomerize and most likely

have the same configuration as in the gas phase. . Platinum is known[1]

to be a poor catalyst for the isomerization of the butenes.

1,3-butadiene can exist in the syn or anti configurations;

$$ =\!\!\diagdown\!\!= \text{(anti)} \longleftrightarrow \diagdown\!\!\_\!\!/\!/ \text{(syn)} $$
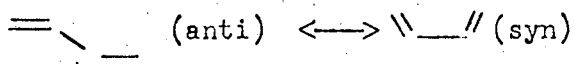
In the gas phase it consists almost entirely[19] as the anti conformer

since rotation about the C-C single bond is hindered by steric repulsion

of the vinyl groups in the syn conformer. However there is no guarantee

that the surface concentrations are the same as for the gas since inter-

conversion between the two conformers may take place via the formation

of the mono-π-adsorbed diene. Using the model by Bond,[17] if butadiene

is chemisorbed as the syn conformer both π-bonds of the adsorbate molecule

can interact similarly with surface metal atoms. This is illustrated in

Fig. 7 where, for simplicity, the C-C bond lengths are drawn as equal.

The work function decrease is approximately twice that observed with

ethylene. However, the surface coverage should be somewhat less than 1/2.

The relatively greater decrease in work function with butadiene might be

explained by 1) the possible delocatization of the π-electrons over the

four carbon atoms which could result in a more efficient transfer of

electrons to the substrate or 2) there is less possibility of back donation

to the antibonding orbitals of the olefinic bond due to the structure of

the adsorbed molecule.

The C(2×2) surface structure generated by chemisorption of C_2H_2

indicates that the adsorbed species are packed in a similar arrangement as

for ethylene (Fig. 5(b)), with $\theta = 1/2$. However, the measured decrease

in work function is considerably larger for acetylene chemisorption suggest-

ing the simultaneous interaction of the two π-bonds with surface orbitals.

In order to illustrate chemisorption on the (111) substrate, it will

again be assumed (for lack of a more complete molecular orbital description)

that an adsorbate molecule bonds to one surface metal atom. Figure 8

then illustrates the close packing of ethylene on the Pt(111) surface

(cf. Fig. 5(b)). Just like on the (100) surface, θ is again 1/2 the

overlap of the Van der Waals envelopes of the ethylene molecules however, must be more severe due to the closeness of the platinum atoms on the (111) surface. A (2x1) unit mesh is proposed and since 60° rotated domains of this structure are equally probable, the LEED pattern indicates a (2x2) surface structure. The decrease in work function is 0.36 V greater than that observed for ethylene on the Pt(100) surface indicating a more efficient overall transfer of electrons from adsorbate to surface. The decrease in work function when propylene chemisorbed on the (111) surface was 0.25 V larger than that measured for ethylene. This difference is very close to that found on the (100) surface and indicates that the coverage of propylene on the (111) surface is again equal to 1/2. This is illustrated in Fig. 9 (cf. Fig. 6). The adsorbate molecules must be packed closely as in row AB or row CD. The (2x2) surface structure observed by LEED signifies that there are surface domains in which one orientation is preferred thus generating domains of structures with (2x1) unit mesh.

Steric considerations indicate that the Pt(111)-(2x2)-(-2-butene)(cis or trans) diffraction patterns cannot result from domains of surface structures with a (2x1) unit mesh; thus formation of a (2x2) unit mesh, Fig. 10 (drawn for trans-2-butene), must be evoked. This more open structure presumably allows the adsorbed molecules to align into an ordered array. The fractional surface coverage is 1/4 and hence the $\Delta\phi$ values for the adsorption of the two butenes are identical within experimental error. By extrapolating the results obtained on the (100) surface, a work function change of around -1.70 V should have been expected for a half-monolayer coverage of the 2-butenes on the (111) substrate. If, as is commonly assumed, $\Delta\phi$ is directly proportional to the coverage, θ, then the measured work function changes indicate a coverage of about 3/8 whereas

a (2×2) unit mesh implies that $\theta = 1/4$. It is possible to pack both trans- and cis-butene more tightly on the (111) surface and to increase the coverage, but the ordered arrays in a closer packed configuration would not give a (2×2) surface strucutre. A (2×2) unit mesh can also be constructed with l-butene in compliance with the observed Pt(111)-(2×2) surface structure; however no work function determination was carried out with this hydrocarbon.

Figure 11 illustrates the packing of 1:3-butadiene on the Pt(111) substrate; once again, the adsorbate is depicted in the syn configuration so that both olefinic bonds can interact with surface metal atoms in a like manner. The unit mesh is (2×2) and the effective coverage is 1/2 thus resembling the packing of chemisorbed ethylene. However, butadiene gives rise to a greater decrease in work function than ethylene similar to the trend observed on the (100) substrate.

Isobutylene was the only hydrocarbon among those which were studied whose chemisorption on the (111) surface did not produce a well-defined surface structure. A (2×2) unit mesh, with $\theta = 1/4$, can be constructed but the closest packing is achieved with the arrangement shown in Fig. 12(a). The coverage is 2/5 and the unit mesh is of dimensions $(\sqrt{7} \times \sqrt{3})$ and rotated $30°$ relative to the substrate unit mesh (transformation matrix $\begin{vmatrix} 1 & -2 \\ 1 & 3 \end{vmatrix}$). The likely diffraction pattern from this surface structure is sketched in Fig. 12(b). The six $(1/5, 1/5)$ order spots around the (00) spots (shown as hatched circles) were in fact observed upon the adsorption of isobutylene indicating a tendency for this molecule to pack as shown in Fig. 12(a). However, the difficulty of achieving such close-packing must be considerable and there should be a substantial amount of disorder in the adsorbate layer. Propylene caused the Pt(111) work function

to decrease by -1.36 V for θ = 0.5 and hence a value of $\Delta\phi$ = -1.09 V

would be expected for θ = 0.4. The presence of a second methyl group

on the same carbon atom (by isobutylene) would presumably increase this

value but, due to disorder in the chemisorbed layer, θ will be somewhat

less than 0.4. Thus the measured $\Delta\phi$ of -1.12 V for isobutylene can be

rationalized.

The only alkyne used in these experiments, acetylene, generated a

(2×2) structure on the Pt (111) surface. The packing presumably resembles

that of ethylene, (Fig. 8), with domains of surface structures with (2×1)

unit mesh and a coverage of 1/2. The measured work function decrease is again

greater than that found with ethylene.

It should be noted that the separation between adsorbed hydrocarbon

molecules, assuming a close packing arrangement may be different from

their intermolecular distance in the solid state. Such close packing

must lead to considerable interactions among the adsorbed molecules which

may influence their structure in the adsorbed state, the observed changes

in work function, and their reactivity on the metal surface.

B. Chemisorption of Carbon Monoxide

Finally, the results obtained using carbon monoxide will be discussed.

It should be emphasized that although the suggested models will explain the

experimental results, they are not unique.

The most commonly assumed configurations of chemisorbed carbon

monoxide on a metal surface are the linear and the bridged forms. The

adsorption of CO in these structures on the (100) surface of a fcc metal can

be described[17] using the molecular orbital description as illustrated

in Fig. 13. The next nearest neighbor distance is the one spanned by the

bridge structure and the t_{2g} orbitals are used for σ-bonding. The linear

species is attached upright to the surface by use of the e_g and t_{2g} orbi-

tals as for an olefin. The experiments clearly indicate that CO adsorbs

on this surface in three bonding states. No comparable models are available

for the interaction of carbon monoxide with the (111) substrate. However,

none of the longer interatomic spacings are available on the (111) surface to

bind CO in the bridge structure. It was found that carbon monoxide is

readily chemisorbed on this surface but only one bonding state was detected.

The most likely model for adsorbed CO on the (111) surface appears to be

the linear form.

Eishens et al.[20] reported that there is a strong single adsorption

band in the infrared spectra of carbon monoxide adsorbed on evaporated

Pt films and this was attributed to the linear structure. Sugita et al.[21]

measured the change in the resistance of a Pt film due to the room tempera-

ture chemisorption of CO and found only one binding state, concluding

that the CO was bound in the linear form. Park and Farnsworth found[22]

that the surface coverage of CO was 1/2 on Ni(100) but one molecule was

adsorbed at each atomic site on the Ni(110) surface.[23] The desorption

temperatures were 500°C for the (100) but only 150°C for the (110) surface,

while the work function increase due to adsorbed CO was less for Ni(100).

These results suggested that CO was bound in a bridge structure on the

Ni(100) face rather than with the linear bond as on the (110) surface.

An interpretation of the Pt(100)-(4x2)-CO surface structure is shown

in Fig. 14(a). The open circles represent the Pt substrate atoms and the

shaded circles represent the CO molecules, each bonded to one platinum

surface atom. The CO, in the α-bound state, is represented as the linear

species since this will presumably be less strongly bound than the bridged

species. The coverage is 3/4 and the work function increase of + 0.18 V

indicates a negative charge on the adsorbate with respect to the adsorbing

metal surface. Due to the positive charge associated with the oxygen

atoms, there must be strong repulsive forces between adjacent adsorbed

molecules. Their separation is $2.8\overset{\circ}{A}$ whereas in solid CO it is $4.1\overset{\circ}{A}$.[*]

Therefore molecules in columns such as A and C might be displaced from

their central positions (as illustrated in Fig. 14(a)), to minimize these

interactions. This could explain why a full monolayer coverage is not

achieved. The difference in bonding strengths of α_1- and α_2-CO is slight

(relevant desorption temperatures being 130°C and 170°C, respectively)

and thus, the adsorbed molecules in rows A and C might well correspond to

α_1-bonded CO. These molecules could thus be removed first by heat treatment

and their desorption would result in the preferential disappearance of the

1/2 order spots in the LEED pattern (Fig. 2a), in accordance with observa-

tion. The extra diffraction spots which are left are streaked, indicating

surface diffusion of the remaining adsorbed molecules to new positions,

and finally the (3×3) surface structure is formed, [Fig. 14(b)]. The

distance of closest approach between adjacent adsorbed molecules is now

the next nearest neighbor distance $(3.9\overset{\circ}{A})$. The coverage is 1/3, roughly

half the room temperature value in accordance with the flash desorption

spectrum and the work function change. The majority of the α_2-CO is

desorbed at substrate temperatures >170°C but a small concentration of

disordered carbon monoxide $(\theta \sim 1/20)$ remains on the surface below 600°C.

---

[*] Eischens[20] found strong interactions in the adsorbed layer for
$\theta > 0.66$.

This β-CO is presumably bound as the bridged structure. The Pt(111)-(4×2)-α-CO surface structure is illustrated in Fig. 15. The coverage is 3/4 and the work function increase is similar to that observed on the (100) surface. However, no displacement of the adsorbate molecules from their upright positions is likely since this will not minimize interactions in the adsorbed layer. The absence of β-CO on the (111) surface directly reflects the absence of longer interatomic spacings.

V. SUMMARY AND CONCLUSIONS

The Pt(111) substrate was characterized by a (1×1) diffraction pattern in contrast to the (5×1) pattern which characterized the Pt(100) orientation. Contamination of both surfaces by carbon, which arose either by diffusion from the bulk crystal or by the cracking of hydrocarbons, was revealed by ring-like diffraction patterns.

Unlike the corresponding paraffins, simple unsaturated gaseous hydrocarbons were readily chemisorbed at pressures $\leq 1\times10^{-7}$ torr and at room temperature on both the Pt(111) and (100) single crystal surfaces. Changes of work function upon adsorption were similar on the two substrates. The binding was weak since the hydrocarbons were desorbed at $\leq 140°C$. The flash desorption spectra contained only one hydrocarbon peak indicating one type of bonding of the adsorbed species on either substrate. The work functions of both metal surfaces were always decreased upon chemisorption indicating a net donation of electrons from the chemisorbed molecule to the substrate. The observed work function changes were generally greater on the (111) surface. The chemisorption of cis-2-butene on the (100) surface did not produce the same work function change as trans-2-butene, indicating that the isomers remained distinct in the adsorbed state. All

gases used, with the exception of isobutylene, removed the Pt(100)-(5x1)

surface structure, the latter returning once the hydrocarbon had been

desorbed from the surface. Ordered surface structures were produced by

the chemisorption of ethylene and acetylene on both substrates; a C(2x2)

structure was generated on the (100) surface while an analagous (2x2)

structure appeared on the (111) surface. The Pt(111)-(2x2) structure was

also produced by propylene, cis-2-butene, trans-2-butene, 1-butene and

1:3-butadiene. Isobutylene did not adsorb into this surface structure

but appeared to exhibit long range order on the Pt(111) surface. However, no

ordering in the adsorbed layer of these hydrocarbons on the Pt(100) surface

was detected. This was the major distinction between the adsorption

characteristics of the two substrates. This difference can be explained

by assuming that there is only one type of adsorption site available on

either substrate to which the hydrocarbon molecule is attached in the

correct orientation to obtain the closest packing. The subtle feature

is that if the carbon atoms maintain their sp^2 hybridization and hence

their bond angle of ~120°, then such close packing on the (111) substrate

must give rise to a preferred arrangement of the adsorbed molecules

which results in an ordered structure due to the three-fold symmetry of the

(111) surface; the two-fold symmetry of the (100) surface permits the

adsorption of the different hydrocarbons in several arrangements; all of

which are equally probable and lead to the same surface coverage. Thus,

ordering of the adsorbed molecules into one type of surface structure

on the (100) surface does not take place. These arguments imply that the

structure of the gaseous hydrocarbon molecule remains vitually unchanged

upon adsorption.

A (4×2) surface structure was generated by the room temperature chemisorption of carbon monoxide on both the Pt(100) and Pt(111) substrates. Simultaneously, small increase in the work function of either surface was measured. However, the interaction of the LEED beam with the (100) surface gradually transformed the (4×2) surface structure of carbon monoxide into a (3×3) structure; no transformation occurred on the Pt(111) surface. Three bonding states of CO were detected on Pt(100); 1) α_1-CO which desorbed at 130°C, 2) α_2-CO which generated the (3×3) surface structure and desorbed at 170°C and 3) a small amount of disordered β-CO below 600°C. The only $m/e = 28$ peak in the flash desorption spectrum from the (111) surface was observed at 170°C (α-CO). These results are best interpreted by assuming that α-CO is the linear form while β-CO corresponds to a bridged structure.

REFERENCES

1. G. C. Bond and P. B. Wells, Adv. in Catalysis, 15, 91 (1964).

2. H. B. Lyon and G. A. Somorjai, J. Chem. Phys. 46, 2539 (1967).

3. C. W. Tucker, Surface Sci. 2, 516 (1964).

4. A. E. Morgan and G. A. Somorjai, Surface Sci. 12, 405 (1968).

5. C. C. Chang, Ph.D. Dissertation, Cornell University (1967), p. 131.

6. R. L. Park and H. H. Madden, Surface Sci. 11, 188 (1968).

7. D. G. Fedak and N. A. Gjostein, Acta Met. 15, 827 (1967).

8. P. W. Palmberg and T. N. Rhodin, Phys. Rev. 161, 586 (1967).

9. P. W. Palmberg, Proceedings of the Fourth International Materials Symposium, Berkeley, California, June 1968 (to be published).

10. P. W. Palmberg and T. N. Rhodin, J. Appl. Phys. 39, 2425 (1968).

11. D. G. Fedak and N. A. Gjostein, Surface Sci. 8, 77 (1967).

12. D. G. Fedak, T. E. Fischer and W. D. Robertson, J. Appl. Phys. 39, 5658 (1968).

13. B. D. Campbell and W. P. Ellis, Surface Sci. 10, 118 (1968).

14. J. J. Lander, Progr. Solid State Chem. 2, 54 (1965).

15. G. C. Bond, Catalysis by Metals, (Academic Press, New York, 1962).

16. G. C. Bond, Platinum Metals Rev. 10, 87 (1966).

17. G. C. Bond, Disc. Faraday Soc. 41, 200 (1966).

18. D. A. Dowden, J. Res. Inst. Catalysis, Hokkaido Univ. 14, 1 (1966).

19. L. B. Smith and J. L. Masingill, J. Amer. Chem. Soc. 83, 4301 (1961).

20. R. P. Eischens, S. A. Francis and W. A. Pliskin, J. Chem. Phys. 194, 194 (1956).

21. T. Sugita, S. Ebisawa and K. Kawasaki, Surface Sci. 11, 159 (1968).

22. R. L. Park and H. E. Farnsworth, J. Chem. Phys. 43, 2351 (1965).

23. R. L. Park and H. E. Farnsworth, J. Appl. Phys. 35, 2220 (1964).

Table I. Structures formed on the Pt(100) and Pt(111) Surfaces and the change in work function, $\Delta\phi$, by gaseous chemisorption

	Pt(100)-(5x1)		Pt(111)-(1x1)	
	$\Delta\phi$ (V)	structure	$\Delta\phi$(V)	structure
CO	+ 0.18	(4x2)	+ 0.17	(4x2)
	+ 0.08	(3x3)		
C_2H_2	- 1.13	c(2x2)	- 1.40	(2x1)[a]
C_2H_4	- 0.75	c(2x2)	- 1.11	(2x1)[a]
C_3H_6	- 1.03	(1x1)	- 1.36	(2x1)[a]
cis-2-butene	- 1.34	(1x1)	- 1.31	(2x2)
trans-2-butene	- 1.12	(1x1)	- 1.32	(2x2)
1,3-butadiene	- 1.61	(1x1)	- 1.62	(2x2)
isobutylene	- 1.01	none	- 1.12	$(\sqrt{7} \times \sqrt{3}\text{-}30°?)$

[a] The diffraction pattern indicates a (2x2) surface structure due to the presence of 60° rotated (2x1) domains.

FIGURE CAPTIONS

Fig. 1 Diffraction patterns of the (111) and (100) surfaces of platinum exhibiting the a) Pt(111)-(1×1) and the b) Pt(100)-(5×1) structures

Fig. 2 Schematic representations of the a) Pt(100)-(4×2)-CO and the b) Pt(100)-(3×3)-CO diffraction patterns.

Fig. 3 Schematic representation of the Pt(111)-(4×2)-CO diffraction pattern.

Fig. 4 Schematic representation of the a) Pt(111)-(2×2)-(C_2H_4) and the b) Pt(100)-c(2×2)-(C_2H_4) diffraction patterns.

Fig. 5a Bonding of ethylene to the Pt(100) surface.

Fig. 5b The Pt(100)-c(2×2)-(C_2H_4) surface structure.

Fig. 6 The random close-packed arrangement of propylene on the Pt(100) surface.

Fig. 7 The random close-packed arrangement of 1,3-butadiene on the Pt(100) surface.

Fig. 8 The Pt(111)-(2×1)-(C_2H_4) surface structure.

Fig. 9 The Pt(111)-(2×1)-(C_3H_6) surface structure.

Fig. 10 The Pt(111)-(2×2)-(trans-2-butene) surface structure.

Fig. 11 The Pt(111)-(2×2)-(1,3-butadiene) surface structure.

Fig. 12a The Pt(111)-($\sqrt{7} \times \sqrt{3}$-30°) - (isobutylene) surface structure.

Fig. 12b Schematic representation of the corresponding diffraction pattern.

Fig. 13 Bonding of carbon monoxide to the Pt(100) surface in a a) bridge structure and b) linear form.

Fig. 14a   The Pt(100)-(4×2)-(α_1-CO) surface structure.

Fig. 14b   The Pt(100)-(3×3)-(α_2-CO) surface structure.

Fig. 15   The Pt(111)-(4×2)-CO surface structure.
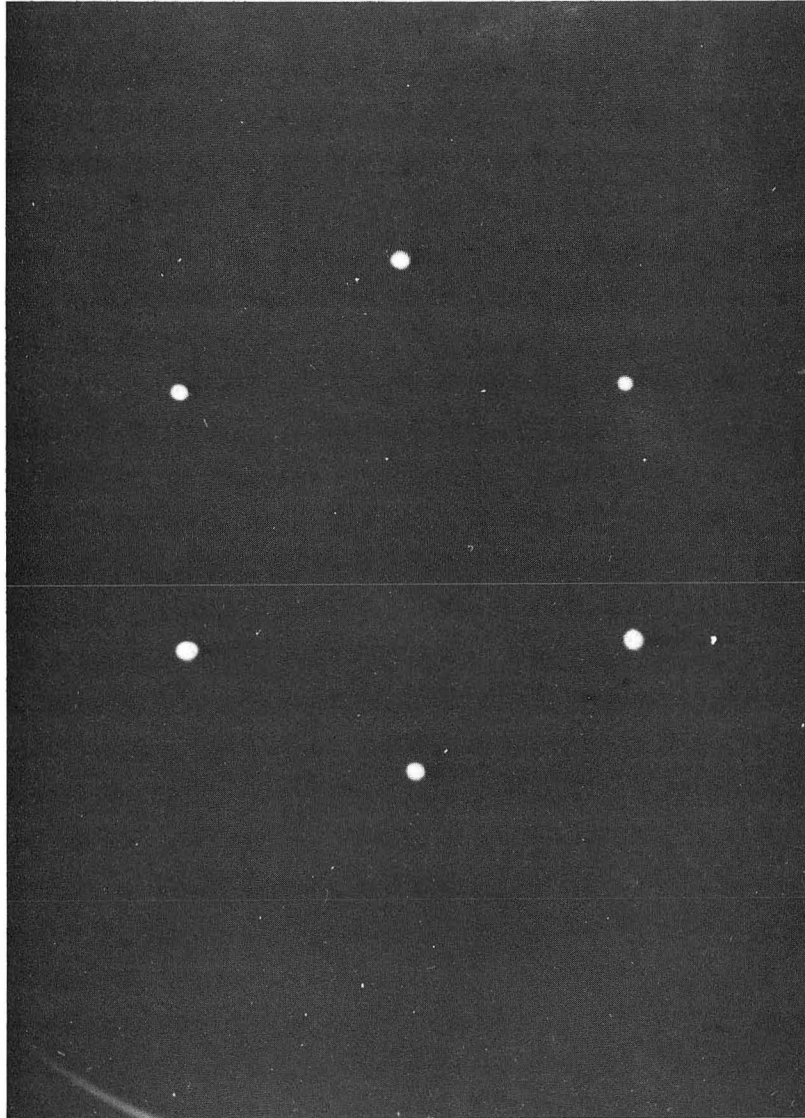
XBB 693-1972

Fig. 1a
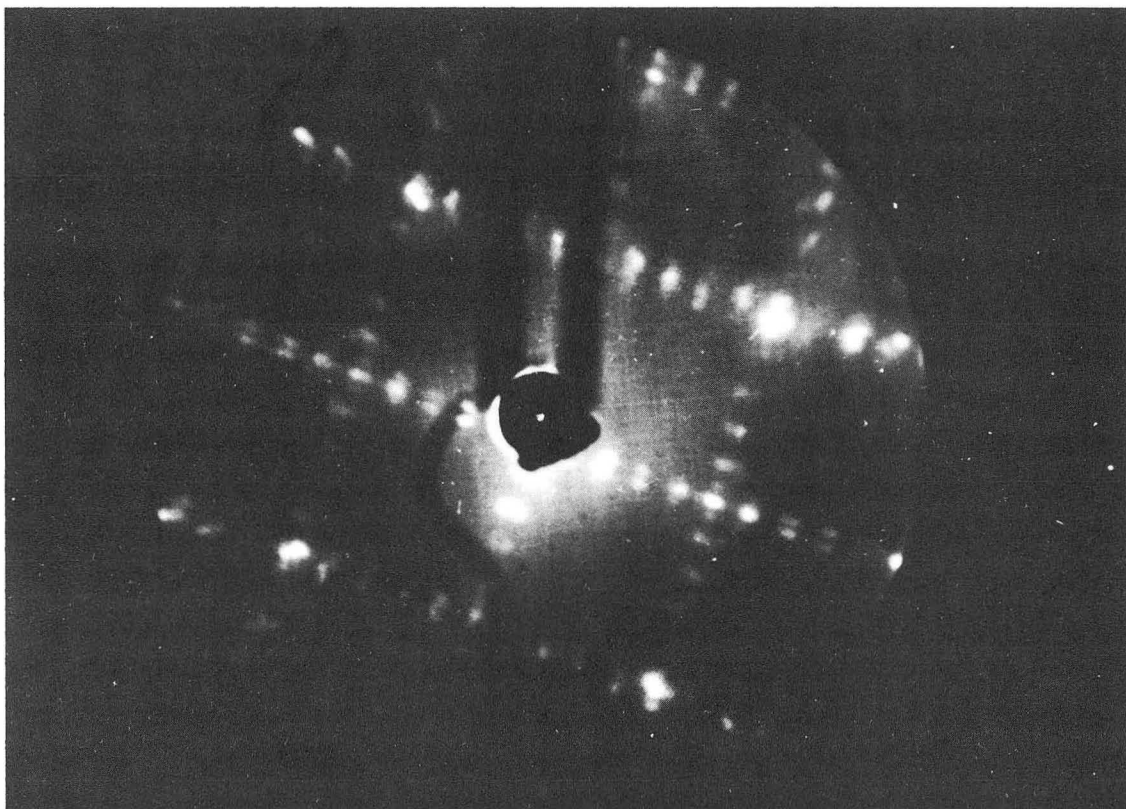
XBB 693-1973

Fig. 1b
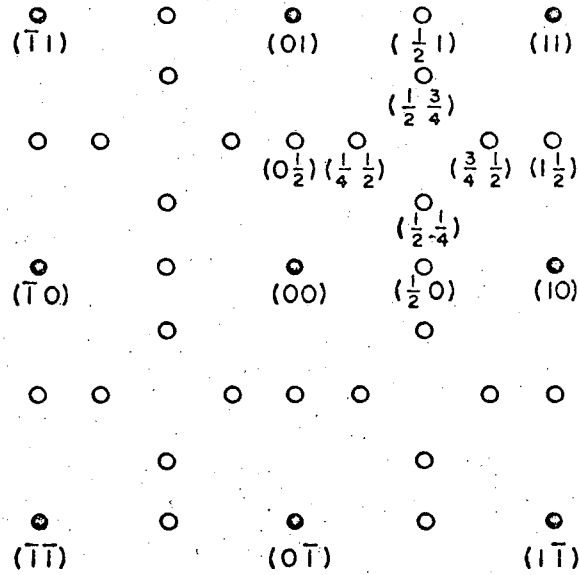
(a)
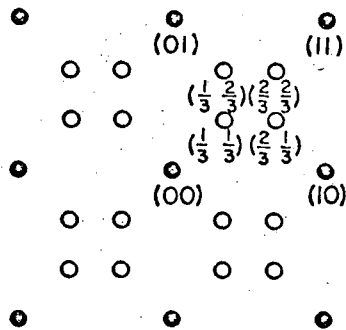
(b)

XBL 693-318

Fig. 2
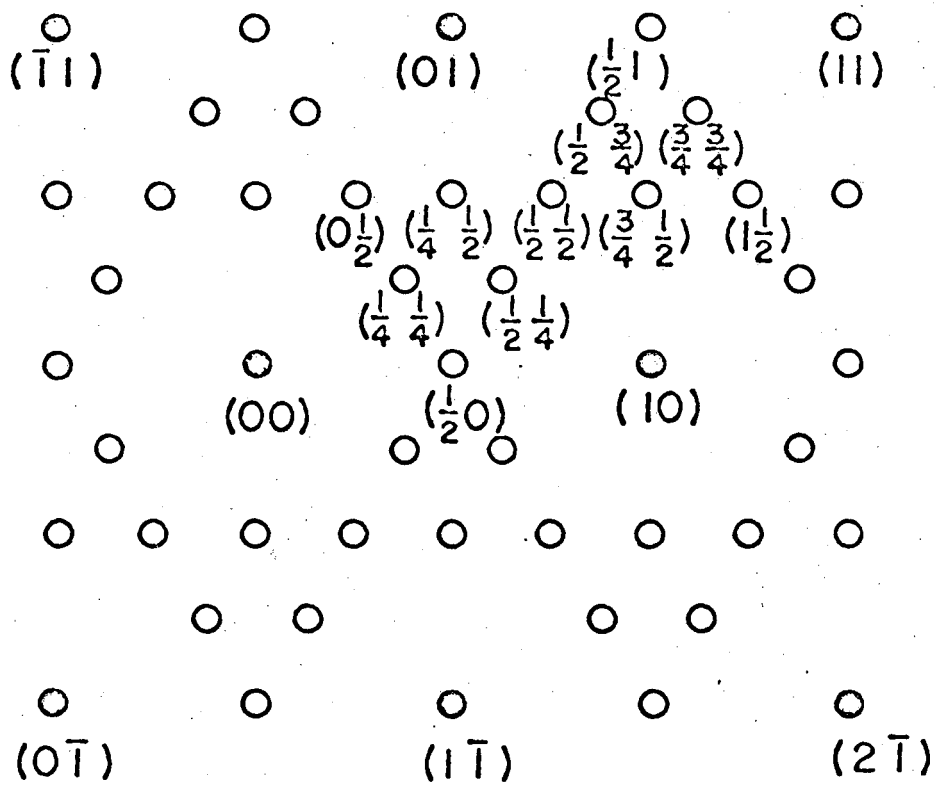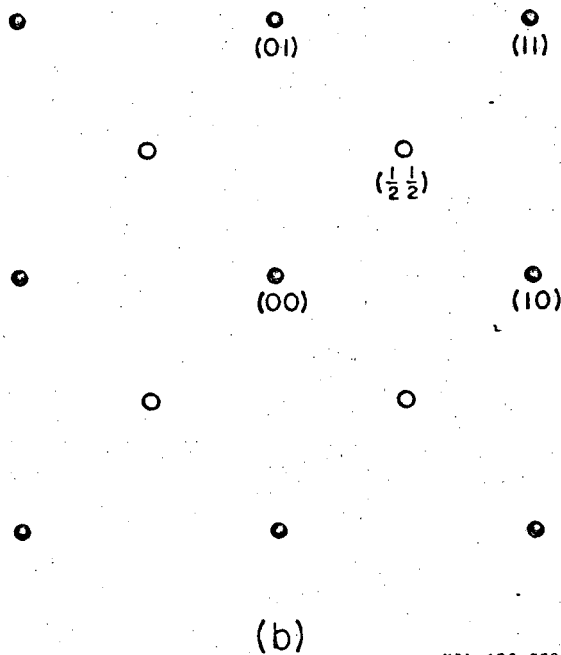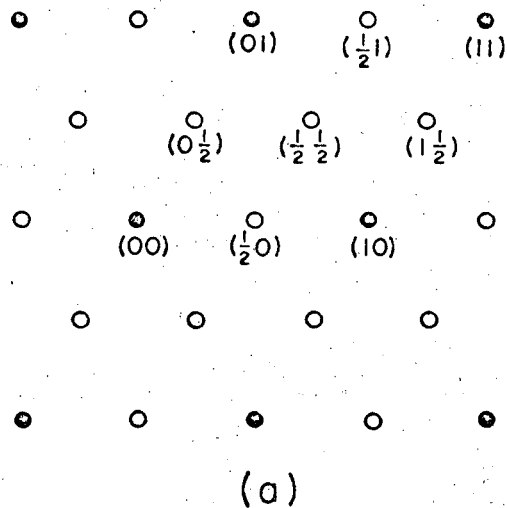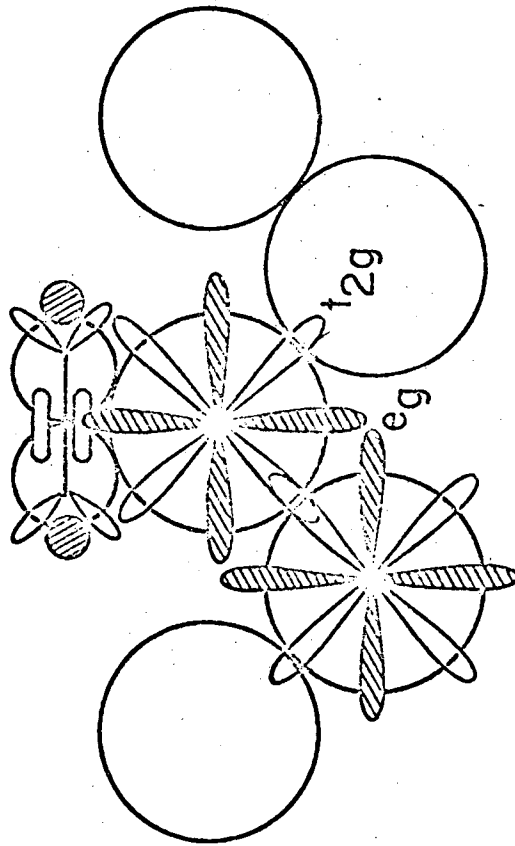
$(\bar{1}1)$ $(0\bar{1})$ $(\tfrac{1}{2}1)$ (11)

$(\tfrac{1}{2}\tfrac{3}{4})$ $(\tfrac{3}{4}\tfrac{3}{4})$

$(0\tfrac{1}{2})$ $(\tfrac{1}{4}\tfrac{1}{2})$ $(\tfrac{1}{2}\tfrac{1}{2})$ $(\tfrac{3}{4}\tfrac{1}{2})$ $(1\tfrac{1}{2})$

$(\tfrac{1}{4}\tfrac{1}{4})$ $(\tfrac{1}{2}\tfrac{1}{4})$

(00) $(\tfrac{1}{2}0)$ (10)

$(0\bar{1})$ $(1\bar{1})$ $(2\bar{1})$

XBL 693-319

Fig. 3

(a)

(b)

XBL 693-320

Fig. 4

Fig. 5a
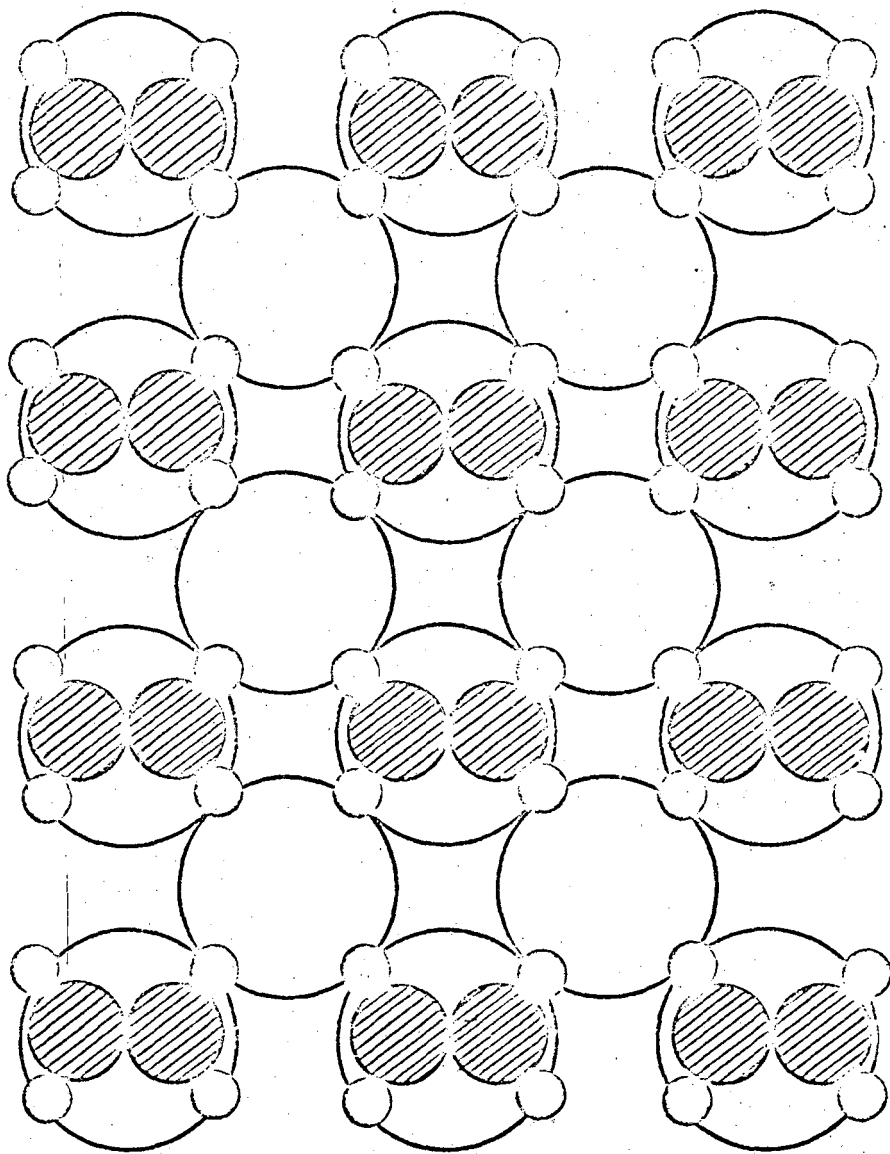
XBL 693-2202

XBL 693-2216

Fig. 5b
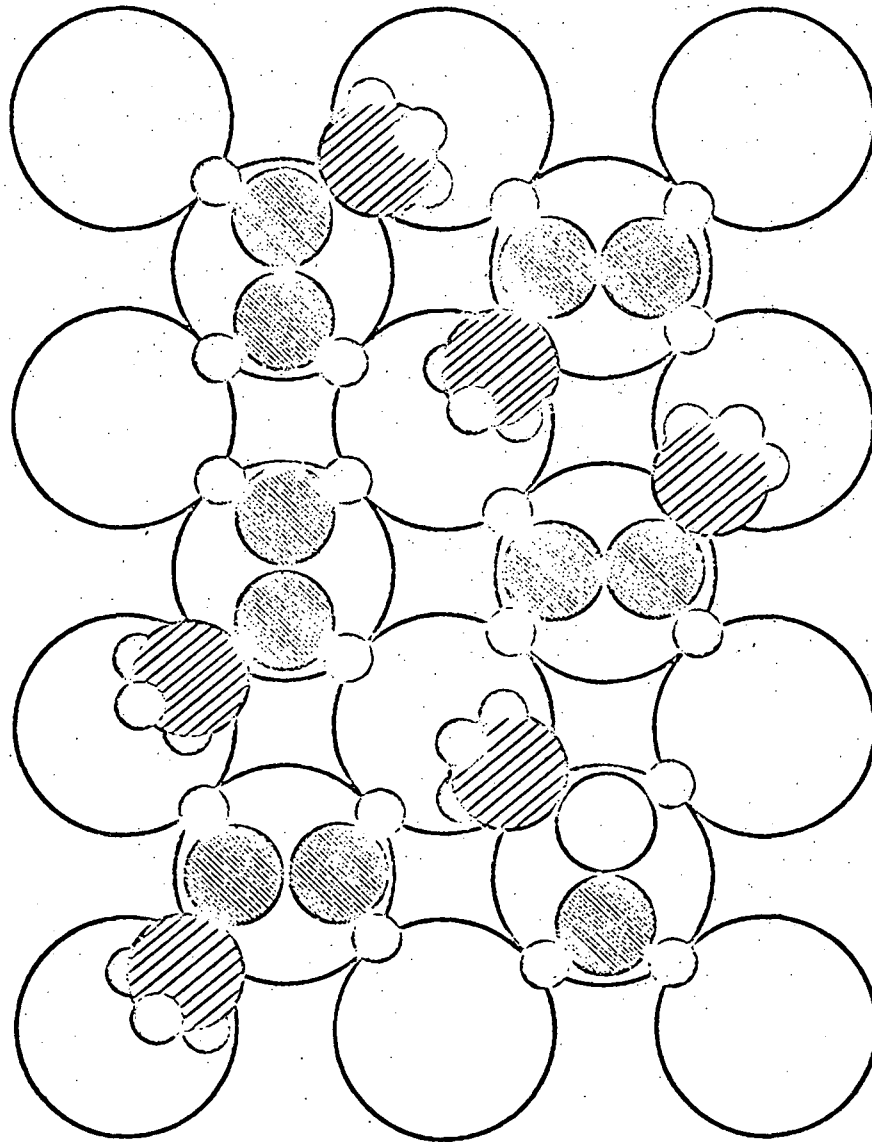
Fig. 6
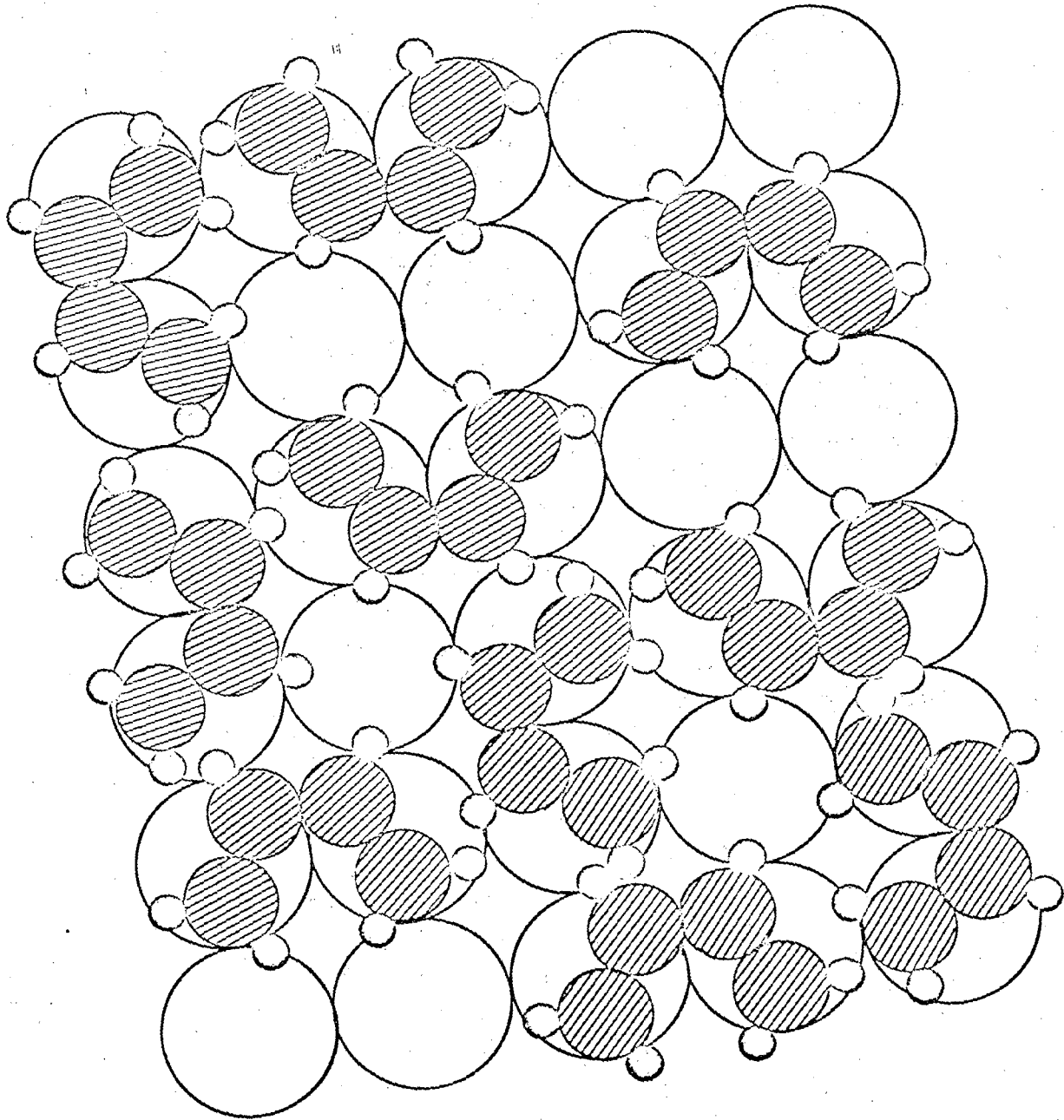
XBL 693-2201

Fig. 7
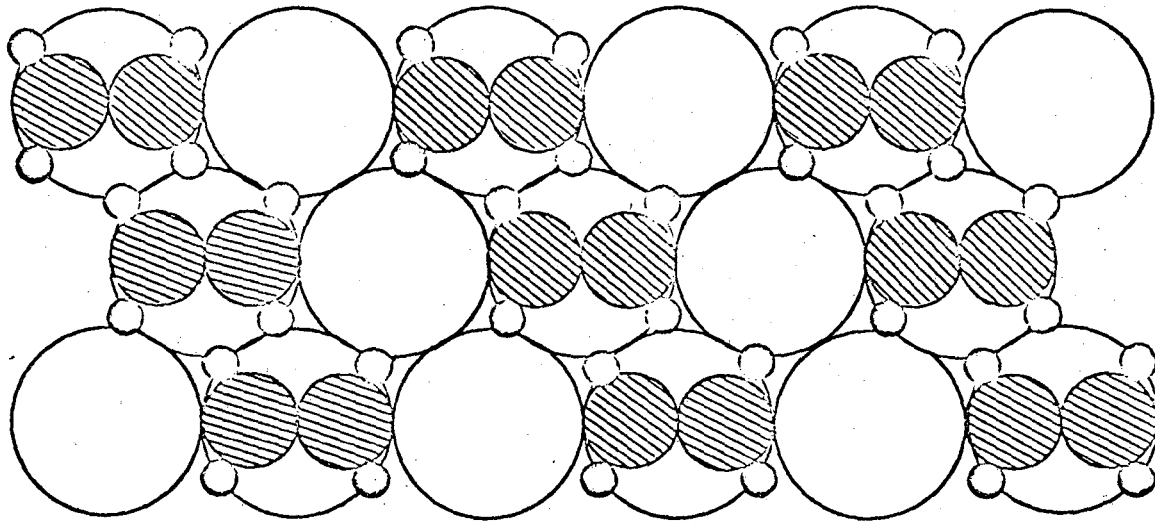
XBL693-2178

Fig. 8
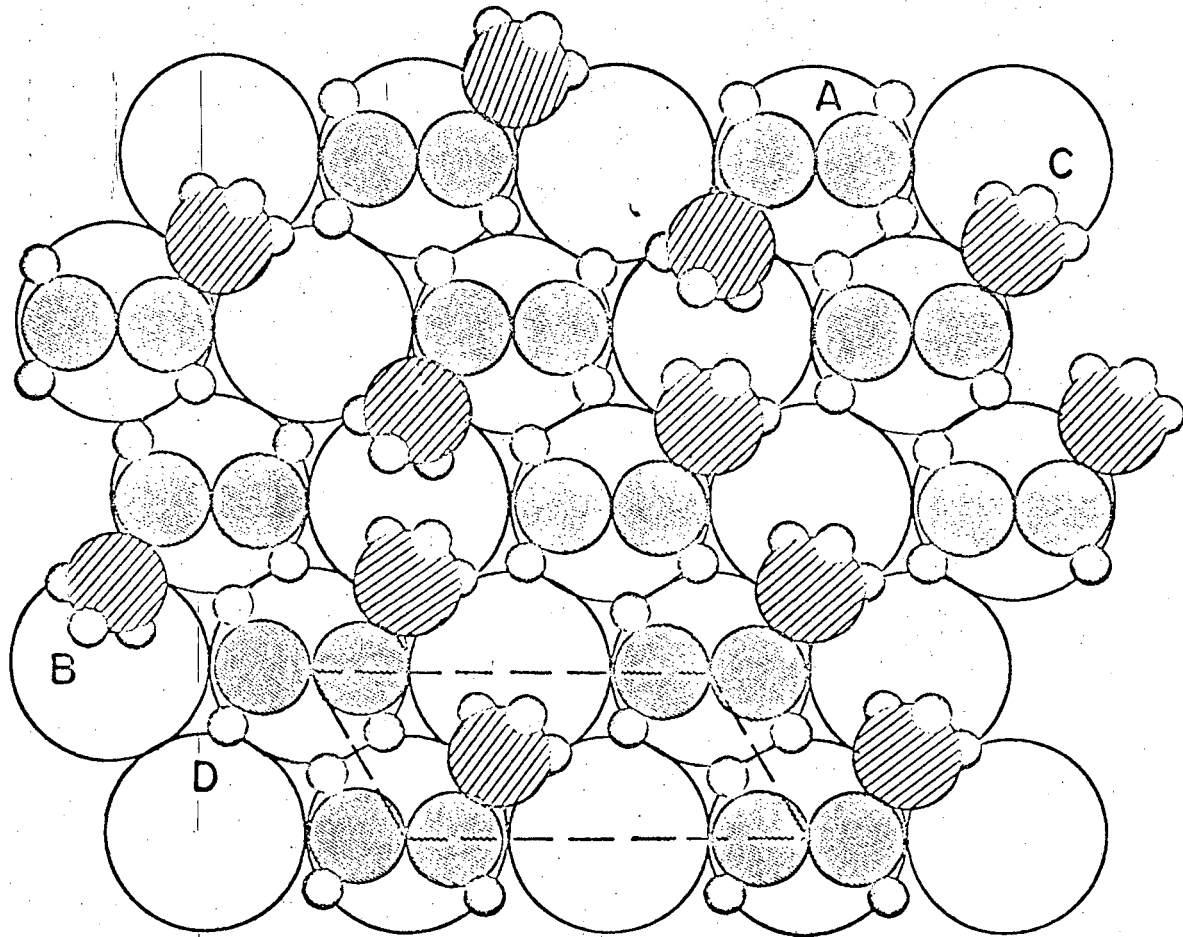
Fig. 9

XBL693-2179

XBL693-2175

Fig. 10

Fig. 11

(01)

$(\frac{2}{5}\frac{2}{5})$

$(\frac{1}{5}\frac{1}{5})(\frac{2}{5}\frac{1}{5})(\frac{3}{5}\frac{1}{5})$

(00)

(10)

(b)

(a)
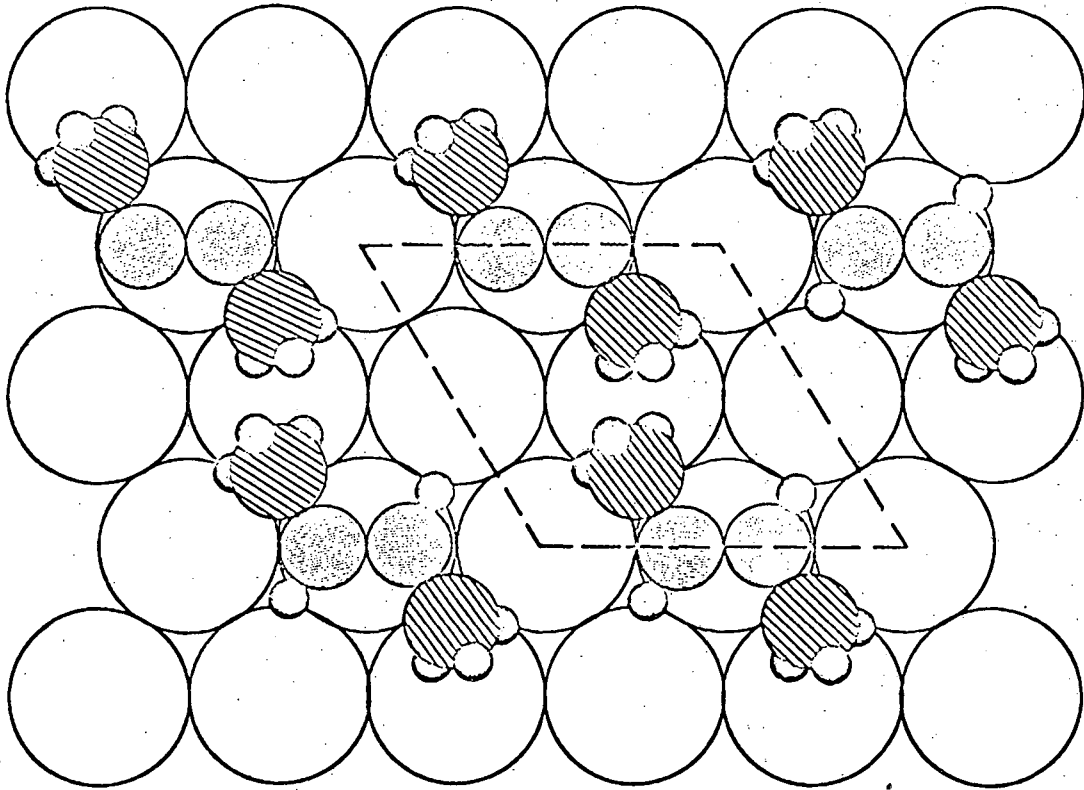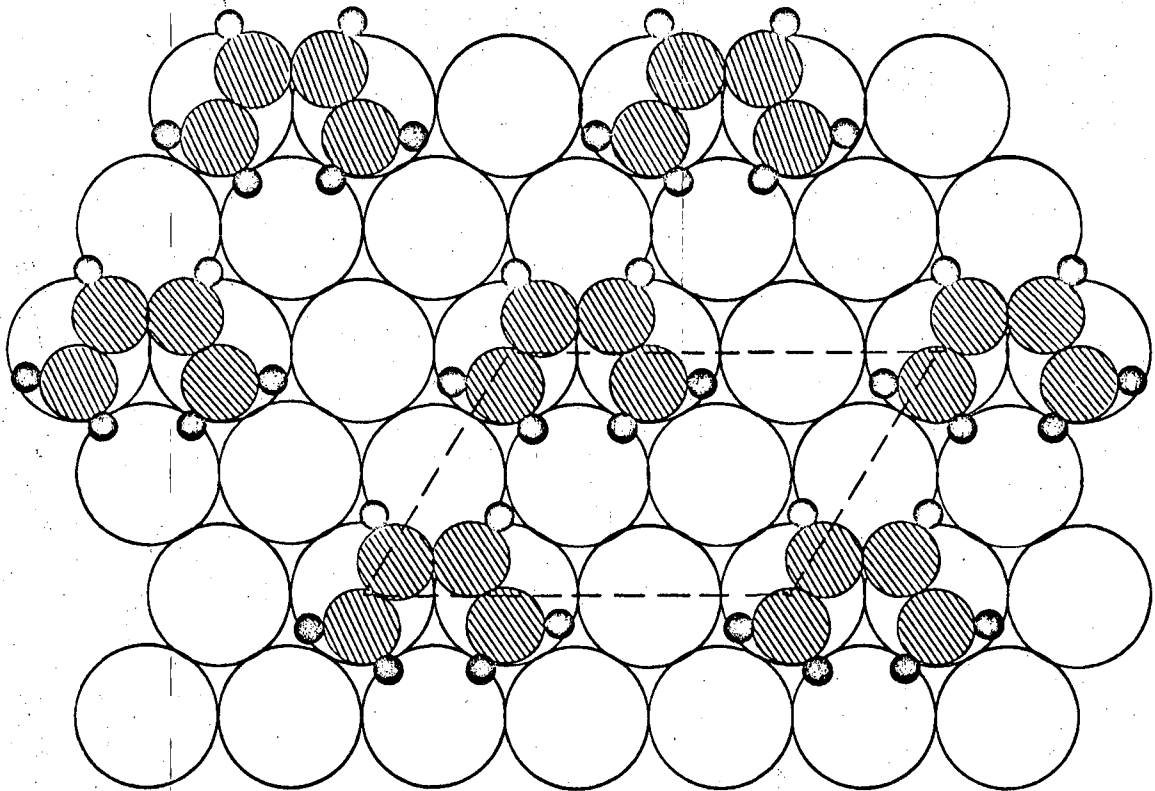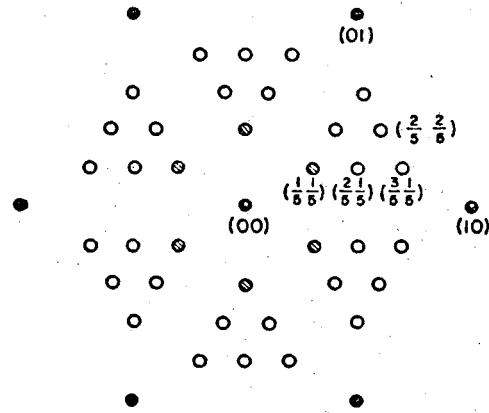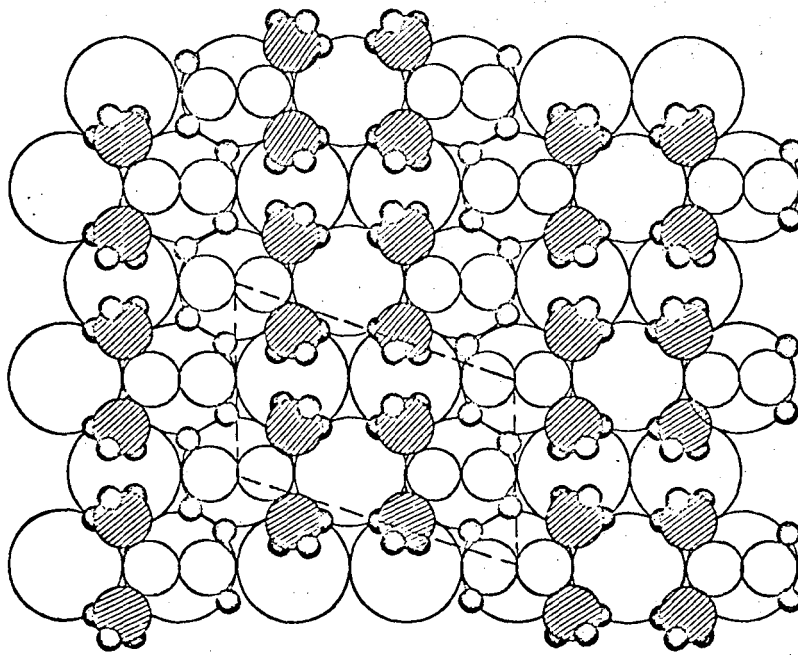
X8L693-2176

Fig. 12
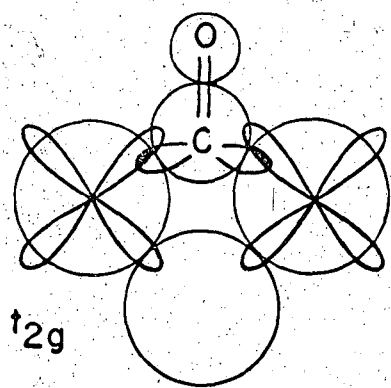
(a)
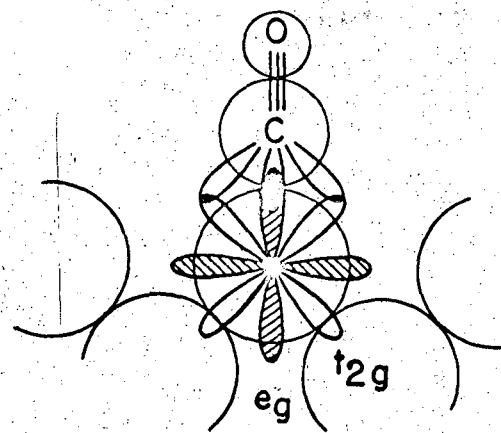
(b)

XBL693-2177

Fig. 13
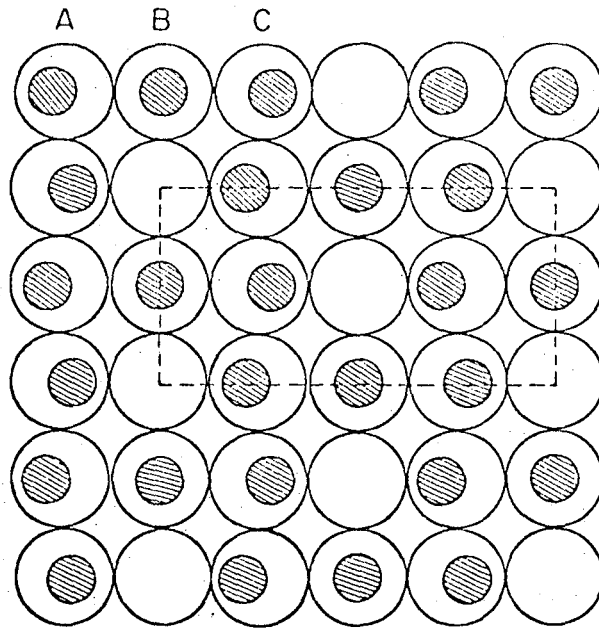
(a)
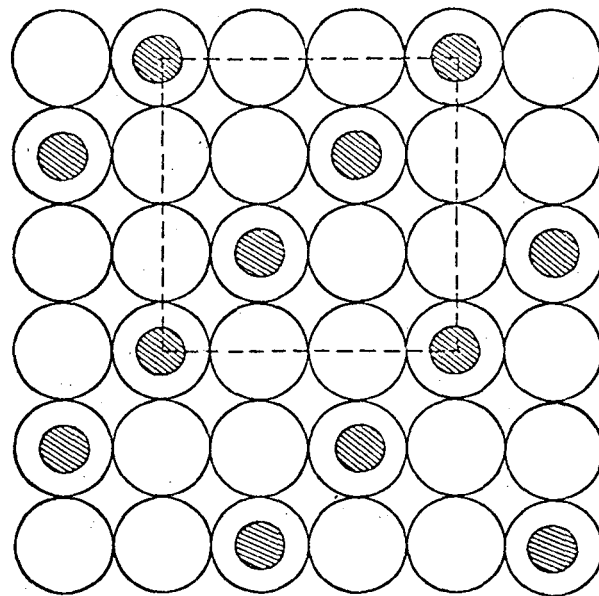
(b)

XBL 693-321

Fig. 14

XBL 693-322

Fig. 15